Polarization-analysis study of the atomic and spin-pair correlations in $Ni_{0.76}Mn_{0.24}$

J. W. Cable and R. M. Nicklow
Oak Ridge National Laboratory, Solid State Division, Oak Ridge, Tennessee 37831

Y. Tsunoda
Faculty of Science, Osaka University, Toyonaka, Osaka, 560 Japan
(Received 4 May 1987)

Neutron diffuse scattering measurements were made on single-crystal $Ni_{0.76}Mn_{0.24}$ to determine the atomic and spin-pair correlations in the reentrant spin-glass state. The nuclear and magnetic diffuse scattering were separated by polarization analysis at $T=10$ K in a field of 8.1 kOe applied parallel to **Q**. The nuclear cross section shows diffuse peaks at (100) and (110) due to atomic short-range order (ASRO) with a range of about $3a_0$. The ASRO parameters for this quenched alloy were determined to 16 shells; these show a preference for like even-shell and unlike odd-shell neighbors. In the experimental geometry, the magnetic cross section determines the correlations between spin components transverse to the applied field, or magnetization direction. The magnetic short-range-order parameters alternate in sign for the first four shells and then remain positive at larger distances. This unusual result corresponds to the coexistence of short-range antiferromagnetic order with both short- and long-range ferromagnetic order.

INTRODUCTION

Disordered $Ni_{1-c}Mn_c$ alloys exhibit magnetic behavior characteristic of competing interaction systems.[1] The Ni-rich alloys are ferromagnetic with a spontaneous magnetization that initially increases with Mn content, reaches a maximum near $c=0.10$, and then rapidly decreases to zero near $c=0.25$.[2-4] Antiferromagnetic order develops for $c \geq 0.32$,[5] but this can be transformed into ferromagnetism by atomic ordering which eliminates most of the Mn-Mn nearest-neighbor pairs.[3] This behavior is attributed to antiferromagnetic nearest-neighbor interactions for the Mn-Mn atom pairs and ferromagnetic interactions for the Ni-Ni and Ni-Mn atom pairs. Clearly, the magnitudes of these interactions are such that they tend to cancel in the $c=0.25$ region for the disordered alloys. It is not surprising that the first observation[6] of the unidirectional field cooling effects now associated with the spin-glass state was made for alloys in this critical concentration region. The presence of these competing interactions yields high-field magnetizations which do not saturate up to 400 kOe.[7] The high-field susceptibility peaks near $c=0.25$ with a value of about 2×10^{-3} emu/mole.

Interest in this system was renewed by recent magnetization studies[8-11] which showed reentrant behavior, i.e., the high-temperature paramagnetic to ferromagnetic transition is followed at lower temperature by a transition to a spin-glass state. The reentrant state appears to be a mixed state with both spin-glass characteristics and a spontaneous ferromagnetic moment. This mixed state interpretation is supported by inelastic neutron measurements[12] which show the presence of long-wavelength spin waves in both the ferromagnetic and the reentrant state. Both the spin-wave stiffness and the transverse susceptibility were found to increase in the reentrant state.

Small-angle neutron scattering measurements[13,14] on these alloys in the presence of an applied field reveal some very unusual effects. In zero field, there is intense diffuse scattering centered at $Q=0$, as would be expected for ferromagnetic clusters. When the field is applied, the overall intensity decreases rapidly and a peak in $I(Q)$ is observed at finite Q. This peak shifts out in Q and becomes less intense with increasing field but persists for fields up to at least 8 kOe at $T=10$ K. This structure in $I(Q)$ corresponds to correlations between spin components that are mostly transverse to the applied field direction. These correlations are for large spatial dimensions ranging from $2\pi/Q^{\max}\simeq500$ Å at 2 kOe to ~80 Å at 8 kOe, and may correspond to intercluster correlations.

All of these results show an unusually complex magnetic behavior for the reentrant state of the disordered Ni-Mn alloys. We decided that a neutron diffuse scattering study of the atom-pair and spin-pair correlations in these alloys would provide additional insight into this complex behavior.

EXPERIMENT

The expected monotonic cross sections for nuclear disorder and paramagnetic scattering are of the same magnitude for Ni-Mn alloys near $c=0.25$. Polarization analysis was therefore chosen as the best method for separation of the nuclear and magnetic scattering. Here, the neutron polarization is maintained either parallel or antiparallel to the scattering vector by use of a guide field at the sample and a neutron spin flipper. The diffuse scattering intensity is measured for both polarizations of the incident beam, and the magnetic scattering appears in the spin-flip intensity, while the nuclear

scattering is non-spin-flip. The measurements were made on the HB-1 triple-axis spectrometer at the high-flux-isotope reactor (HFIR) at the Oak Ridge National Laboratory (ORNL). The spectrometer was set for elastic scattering at 71.8 meV with $^{57}FeSi$ as both the monochromator and analyzer and with 40′ collimation before and after the sample.

The measurements were made on a single crystal of $Ni_{0.76}Mn_{0.24}$ with a volume of approximately 1.5 cm^3. The crystal was grown by the Bridgman method, annealed at 970 °C for 22 h, and then water quenched. The magnetic field and temperature conditions were maintained by use of a Displex refrigerator for which the tailpiece was located in the gap of a horizontal field electromagnet. Depolarization of the beam by the sample was observed below T_c. This was quite severe at low fields and sufficiently sharp at 100 Oe to establish $T_c = 240$ K. An applied field of 8.1 kOe was required to retain 90% of the beam polarization through the sample at 10 K, and most of the data were taken under these H and T conditions. The intensities were corrected for background and converted to absolute cross sections by calibration against vanadium. The resulting cross sections were then corrected for the imperfections in the various polarizing components of the spectrometer to obtain the actual spin-flip and non-spin-flip cross sections. The results for the first Brillouin zone of an (001) orientation are shown in Figs. 1 and 2 in the form of isointensity (actually cross section) contours. The non-spin-flip cross section shown in Fig. 1 contains the nuclear disorder scattering (~0.36 b monotonic), plus the isotopic incoherent scattering from the Ni atoms (~0.30 b), and one third of the spin incoherent scattering from the Mn atoms (~0.01 b). The latter effects are isotropic so the diffuse peaks at (100) and (110) are associated with the nuclear disorder. These peaks show the presence of

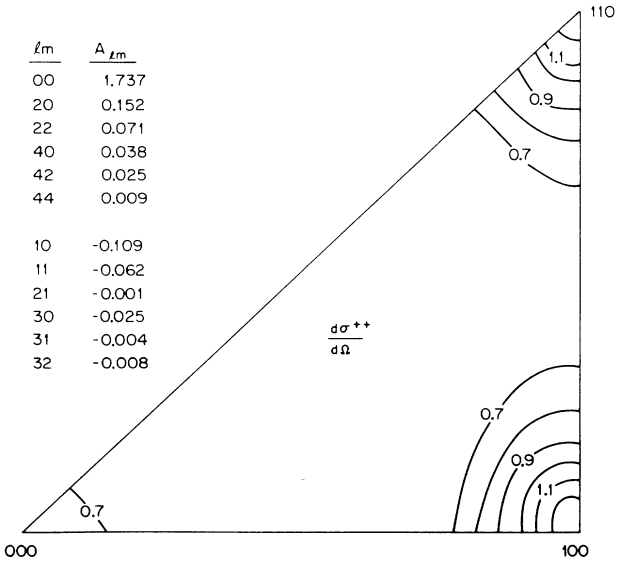

FIG. 1. Isointensity contours of the non-spin-flip cross section, $d\sigma^{++}/d\Omega$, for $Ni_{0.76}Mn_{0.24}$. Contour levels are in units of ($b\,sr^{-1}at^{-1}$). The A_{lm} are coefficients obtained by Fourier transformation of these data (see the text).

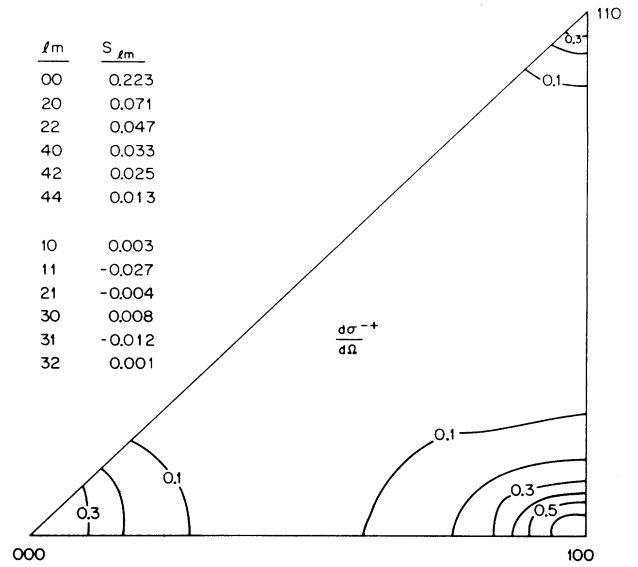

FIG. 2. Isointensity contours of the spin-flip cross section, $d\sigma^{-+}/d\Omega$, for $Ni_{0.76}Mn_{0.24}$. Contour levels are in units of ($b\,sr^{-1}at^{-1}$). The S_{lm} are coefficients obtained by Fourier transformation of these data (see the text).

atomic short-range order (ASRO) of the Cu_3Au type, which is not surprising since Ni_3Mn orders in that structure.

Similar results for the spin-flip cross section are shown in Fig. 2. This cross section contains only the small isotropic contribution from the Mn spin incoherent scattering (~0.02 b) plus the magnetic scattering from those spin components transverse to the applied field direction ($\mathbf{H}\|\mathbf{Q}$). Diffuse peaks are observed at (000), (100), and (110). The low contour levels at (110) and some of the contour shape at (100) can be attributed to the squared magnetic form factor dependence of the scattering which is included in these data.

The temperature dependence of the magnetic short-range-order (MSRO) scattering is shown in Fig. 3. The corrected cross sections near (100) at $T = 10$ K and

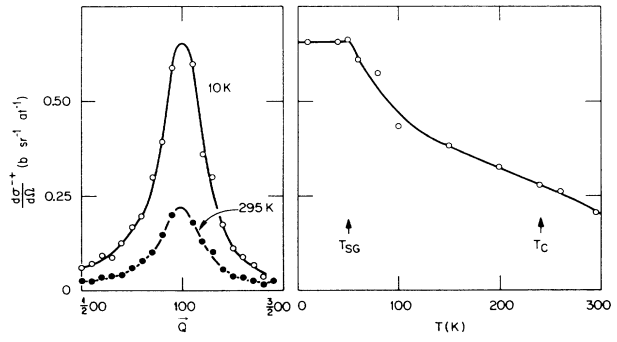

FIG. 3. The spin-flip cross section at (100) at fixed temperatures of 10 and 295 K and the temperature dependence of the peak cross section. T_c is the Curie temperature and T_{SG} is spin-glass phase boundary.

$T=295$ K are on the left of this figure, and the temperature dependence of the peak height cross section is shown on the right. These data pass smoothly through T_c with a cross section that increases continuously down to the spin-glass transition $T_{SG}\simeq 50$ K where it saturates. This evolution of the spin correlations is accompanied by very little change in the half-width of the peak.

ANALYSIS

The nuclear disorder cross section is given by

$$\frac{d\sigma^{++}}{d\Omega}(\mathbf{Q})=c(1-c)(b_{\mathrm{Mn}}-b_{\mathrm{Ni}})^2\sum_{\mathbf{R}}\alpha(\mathbf{R})e^{i\mathbf{Q}\cdot\mathbf{R}}\ , \tag{1}$$

where c is the Mn concentration, $b_{\mathrm{Mn}}=-0.373$, $b_{\mathrm{Ni}}=1.03\times10^{-12}$ cm, and the $\alpha(\mathbf{R})$ are Warren-Cowley short-range-order parameters. The cross section data of Fig. 1 were Fourier transformed to obtain the two-dimensional Fourier coefficients shown in the figure. These are related to the three-dimensional $\alpha(\mathbf{R})$ by $A_{lm}=\sum_n\alpha_{lmn}$, where the atomic positions are given by

$$\mathbf{R}=\tfrac{1}{2}(l\mathbf{a}_1+m\mathbf{a}_2+n\mathbf{a}_3)\ .$$

The A_{lm} for the even shells of atoms are all positive and larger in absolute magnitude than the odd-shell A_{lm} which are all negative. This is to be expected for the Cu_3Au type of order for which $\alpha_{\mathrm{even}}=1$ and $\alpha_{\mathrm{odd}}=-\frac{1}{3}$ when perfectly ordered. The A_{lm} coefficients have significant magnitudes out to A_{44}, which contains contributions from α_{lmn} out to 16 or perhaps 18 shells for a distance of approximately $3a_0$ ($a_0=3.595$ Å). With this persistance of short-range order (SRO) to large distances, there is insufficient information to obtain a unique solution for the even-shell α_{lmn}. However, a reasonable solution can be obtained by setting all α_{lmn} beyond the 18th shell to zero and by constraining the α_{lmn} to decrease with distance. With these restrictions, we obtain the α_{lmn} values listed in Table I. Here, $\alpha_{000}=1.57$ is larger than the expected value of unity because of the inclusion in $d\sigma^{++}/d\Omega$ of the isotropic background contributed by the incoherent scattering. The α_{lmn} for finite R are small and show a preference for unlike odd-shell neighbors and like even-shell neighbors. In terms of the site occupation operator, $p_{\mathbf{R}}$, which counts the number (0 or 1) of Mn atoms at lattice site $\mathbf{R}$, the $\alpha(\mathbf{R})$ can be written as

$$c(1-c)\alpha(\mathbf{R})=\langle(p_0-c)(p_{\mathbf{R}}-c)\rangle\ , \tag{2}$$

where the angular brackets denote a configurational average. The corresponding Mn-Mn atom-pair correlation

$$\langle p_0p_{\mathbf{R}}\rangle=c^2+c(1-c)\alpha(\mathbf{R}) \tag{3}$$

is shown in Fig. 4 as a function of R. The probability of such pairs is c^2 (for $\mathbf{R}\neq0$) in the random alloy, and the pair correlation is higher (lower) than this for the even (odd) shells, at least out to about $3a_0$.

The magnetic cross section is given by

$$\frac{d\sigma^{-+}}{d\Omega}(\mathbf{Q})=\left[\frac{e^2\gamma}{mc^2}\right]^2f^2(Q)\sum_{\alpha\beta}(\delta_{\alpha\beta}-\hat{Q}_\alpha\hat{Q}_\beta)\times\sum_{\mathbf{R}}\langle S_0^\alpha S_{\mathbf{R}}^\beta\rangle e^{i\mathbf{Q}\cdot\mathbf{R}}\ , \tag{4}$$

where α and β are Cartesian components, $\hat{Q}_\alpha$ and $\hat{Q}_\beta$ are direction cosines of $\mathbf{Q}$, $(e^2\gamma/mc^2)=0.539\times10^{-12}$ cm, $f(Q)$ is the magnetic form factor, and $\langle S_0^\alpha S_{\mathbf{R}}^\beta\rangle$ is the configurationally average spin-pair correlation. In the present experiment, the magnetic field (which is parallel to $\mathbf{Q}$) defines the z axis of the spin system. Under these conditions, only the transverse correlations are

TABLE I. ASRO and MSRO parameters for Ni–24-at % Mn.

lmn	α_{lmn}	S_{lmn}
000	1.57	0.15
200	0.067	0.023
220	0.030	0.013
222	0.012	0.008
400	0.014	0.011
420	0.009	0.007
422	0.005	0.005
440	0.003	0.004
600,442	0.003	0.004
110	−0.048	−0.003
211	−0.005	−0.010
310	−0.006	0.006
321	−0.003	0.007
330,411	−0.001	−0.002
332	−0.001	−0.001

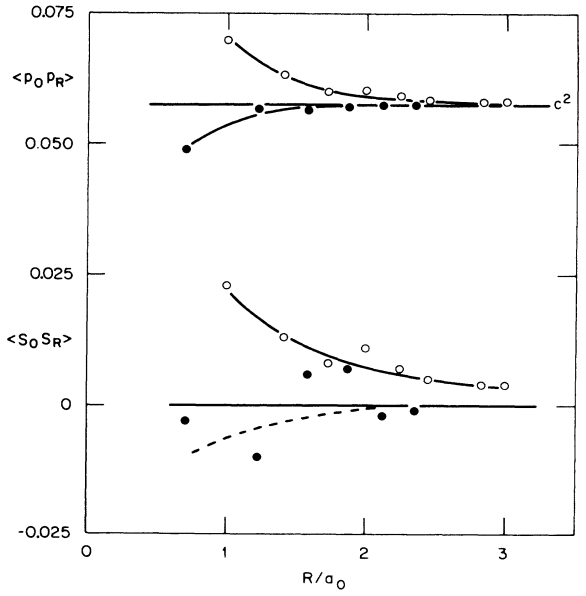

FIG. 4. The R dependence of the atom-pair and spin-pair correlations of $Ni_{0.76}Mn_{0.24}$. Open and filled circles denote even- and odd-shell neighbors, respectively.

observed and the cross section reduces to

$$\frac{d\sigma^{-+}}{d\Omega}(\mathbf{Q})=2\left[\frac{e^2\gamma}{mc^2}\right]^2 f^2(Q)\sum_R \langle S_0^x S_R^x\rangle e^{i\mathbf{Q}\cdot\mathbf{R}} . \quad (5)$$

Since we expect most of the magnetic moment to reside on the Mn atoms, we have used an approximate Mn form factor,

$$f(Q)=\exp[-0.22(h^2+k^2)] ,$$

in Fourier transforming the data of Fig. 2. The Fourier coefficients listed in that figure are given by $S_{lm}=\sum_n S_{lmn}$, where $S_{lmn}=\langle S_0^x S_R^x\rangle$. Here again, the even-shell coefficients are positive and have apparently significant values out to S_{44}, i.e., to the 18th shell. The odd-shell S_{lm} are small with a tendency toward negative values. With the same constraints as those placed on the α_{lmn}, we obtain the S_{lmn} values given in Table I and which are plotted in Fig. 4 as a function of R. The even-shell S_{lmn} are all positive and decrease with R toward the expected value of zero at large R. The odd-shell S_{lmn} are small with negative values for the first and third neighbor shells.

DISCUSSION

Previous neutron results[15] for disordered Ni-Mn alloys show that the average ferromagnetically aligned moment at both the Ni and the Mn sites decreases with increasing Mn content. The Ni moment decreases from 0.58 μ_B/Ni at $c=0.05$ to 0.30 μ_B/Ni at $c=0.20$, while the Mn moment changes from 3.5 μ_B/Mn to 1.1 μ_B/Mn over the same concentration region. This decrease at the Ni sites is presumably a band structure effect and all the Ni sites are expected to have about the same moment. By contrast, the decrease in average Mn moment is largely a local environment effect involving spin reversal for those Mn atoms in Mn-rich nearest-neighbor environments. In the critical concentration region, the ferromagnetic moment averaged over all Mn sites is small, but a large moment remains at each Mn site and there are large Mn moment fluctuations in both the longitudinal and transverse spin components.

This local environment description is also supported by nuclear magnetic resonance (NMR) data[16] which show at least three groups of resonance lines for ^{55}Mn in Ni-Mn alloys. The two higher-frequency lines are associated with Mn atoms with slightly different moments parallel to the net ferromagnetic moment, while the low-frequency line is attributed to Mn atoms with reversed spin. The average hyperfine field for the reversed-spin Mn atoms exhibits[17] a temperature dependence remarkably similar to that shown in Fig. 3 for the (100) cross sections.

In the present experiment, we have determined the spin correlations for those spin components transverse to the applied field direction. The single-site fluctuations are contained in the S_{000} parameter which can be used to obtain the relative magnitudes of the longitudinal and transverse fluctuations. The transverse fluctuation is

$$S_{000}=\langle S_0^x S_0^x\rangle\equiv\langle S_x^2\rangle ,$$

while the longitudinal fluctuation is $\langle S_z^2\rangle-\langle S_z\rangle^2$. The $\langle S_z\rangle$ term is small at this concentration, so the total fluctuation can be described by

$$\langle S_x^2\rangle+\langle S_y^2\rangle+\langle S_z^2\rangle\simeq S(S+1)\simeq cS_{\mathrm{Mn}}(S_{\mathrm{Mn}}+1) ,$$

where all of the spin fluctuation is attributed to the Mn sites. With $S_{\mathrm{Mn}}=2$ and our observed $S_{000}=\langle S_x^2\rangle=\langle S_y^2\rangle=0.15$, we obtain $\langle S_z^2\rangle=1.14$. Thus, most of the single-site fluctuation is longitudinal and not observable in the present experiment. This longitudinal fluctuation was previously measured[15] and attributed to Mn spin reversal.

Small-angle scattering measurements on Ni-Mn alloys in this concentration region show a diffuse peak at $Q=0$ corresponding to ferromagnetic spin correlations extending to large distances.[13,14] Application of a magnetic field extinguishes much of this scattering intensity because the large clusters align with the infinite cluster and the intensity shifts into the Bragg peaks. Nevertheless, some of this diffuse peak remains even in applied fields of $\sim$8 kOe at $T=10$ K. This can also be seen in the present experiment in the form of a diffuse peak at (000) (see Fig. 2). Clearly, there are ferromagnetic spin correlations present in this alloy. In spite of that, the spin-pair correlation, S_{lmn}, for $R\neq 0$ alternates from negative in the odd shells to positive in the even shells out to the fourth neighbor shell (see Table I and Fig. 4). The correlation only becomes ferromagnetic beyond the fourth shell. This is a totally unexpected result which indicates an antiferromagnetic short-range correlation of the transverse spin components to four shells. The type-I antiferromagnetic structure observed in these alloys for $c\geq 0.32$ has spin-pair correlations that are $\frac{2}{3}$ antiparallel and $\frac{1}{3}$ parallel for odd-shell neighbors and all parallel for even-shell neighbors. The present results are consistent with such correlations and suggest that this type of antiferromagnetic short-range order coexists with ferromagnetic long-range and short-range order in these NiMn alloys near the critical concentration for ferromagnetism. The observed temperature dependence of the diffuse scattering shows that these short-range correlations persist to temperatures well above the reentrant phase boundary.

ACKNOWLEDGMENTS

The authors are grateful to J. R. Weir III and T. L. Collins for technical assistance. This research was supported by the Division of Materials Sciences, U.S. Department of Energy under Contract No. DE-AC05-840R21400 with Martin Marietta Energy Systems, Inc.

[1]W. J. Carr, Phys. Rev. **85**, 590 (1952).
[2]S. Kaya and A. Kussman, Z. Phys. **72**, 293 (1931).
[3]G. R. Piercy and E. R. Morgan, Can. J. Phys. **31**, 529 (1953).
[4]H. Tange, T. Tokunaga, and M. Goto, J. Phys. Soc. Jpn. **45**, 105 (1978).
[5]O. Moze, T. J. Hicks, and P. von Blanckenhagen, J. Magn. Magn. Mater. **42**, 103 (1984).
[6]J. S. Kouvel and C. D. Graham, J. Phys. Chem. Solids **11**, 220 (1959).
[7]K. Okuda, H. Mollymoto, and M. Date, J. Phys. Soc. Jpn. **47**, 1015 (1979).
[8]R. G. Aitken, T. D. Cheung, J. S. Kouvel, and H. Hurdequint, J. Magn. Magn. Mater. **30**, L1 (1982).
[9]W. Abdul-Razzaq and J. S. Kouvel, J. Appl. Phys. **55**, 1623 (1984).
[10]W. Abdul-Razzaq and J. S. Kouvel, J. Appl. Phys. **57**, 3468 (1985).
[11]J. S. Kouvel and W. Abdul-Razzaq, J. Magn. Magn. Mater. **53**, 139 (1985).
[12]B. Hennion, M. Hennion, F. Hippert, and A. P. Murani, J. Phys. F **14**, 489 (1984).
[13]M. Hennion, I. Mirebeau, F. Hippert, B. Hennion, and J. Bigot, J. Magn. Magn. Mater. **54-57**, 121 (1986).
[14]M. Hennion, I. Mirebeau, B. Hennion, and S. Lequien, Europhys. Lett. **2**, 393 (1986).
[15]J. W. Cable and H. R. Child, Phys. Rev. B **10**, 4607 (1974).
[16]Y. Kitaoka, K. Ueno, and K. Asayama, J. Phys. Soc. Jpn. **44**, 142 (1978).
[17]H. Yamagata and M. Matsumura (unpublished).